PDCD6 regulates lactate metabolism to modulate LC3-associated phagocytosis and antibacterial defense

Lulu Sun[1, †], Sijin Wu[2, †], Hui Wang[1], Tianyu Zhang[1], Mengyu Zhang[1], Xuepeng Bai[3], Xiumei Zhang[4], Bingqing Li[5], Cai Zhang[6], Yan Li[1], Jun Zhou[1,7]* and Tianliang Li[1]*

[1] Center for Cell Structure and Function, Shandong Provincial Key Laboratory of Animal Resistance Biology, Collaborative Innovation Center of Cell Biology in Universities of Shandong, College of Life Sciences, Shandong Normal University, Jinan 250358, China.
[2] Academy of Pharmacy, Xi'an Jiaotong-Liverpool University, Suzhou, 215123, China.
[3] Department of Cardiac Surgery, Public Health Clinical Center Affiliated to Shandong University, Jinan, 250013, China.
[4] School of Health Care Security, Shandong First Medical University & Shandong Academy of Medical Sciences, Jinan, 250117, China.
[5] Department of Pathogen Biology, School of Clinical and Basic Medical Sciences, Shandong First Medical University & Shandong Academy of Medical Sciences, Jinan, 250117, China.
[6] Institute of Immunopharmacology and Immunotherapy, School of Pharmaceutical Sciences, Shandong University, Jinan 250012, China.
[7] State Key Laboratory of Medicinal Chemical Biology, Haihe Laboratory of Cell Ecosystem, College of Life Sciences, Nankai University, Tianjin, 300071, China.

[†] These authors contributed equally: Lulu Sun, Sijin Wu.

*Correspondence: li.tianliang@outlook.com and junzhou@sdnu.edu.cn

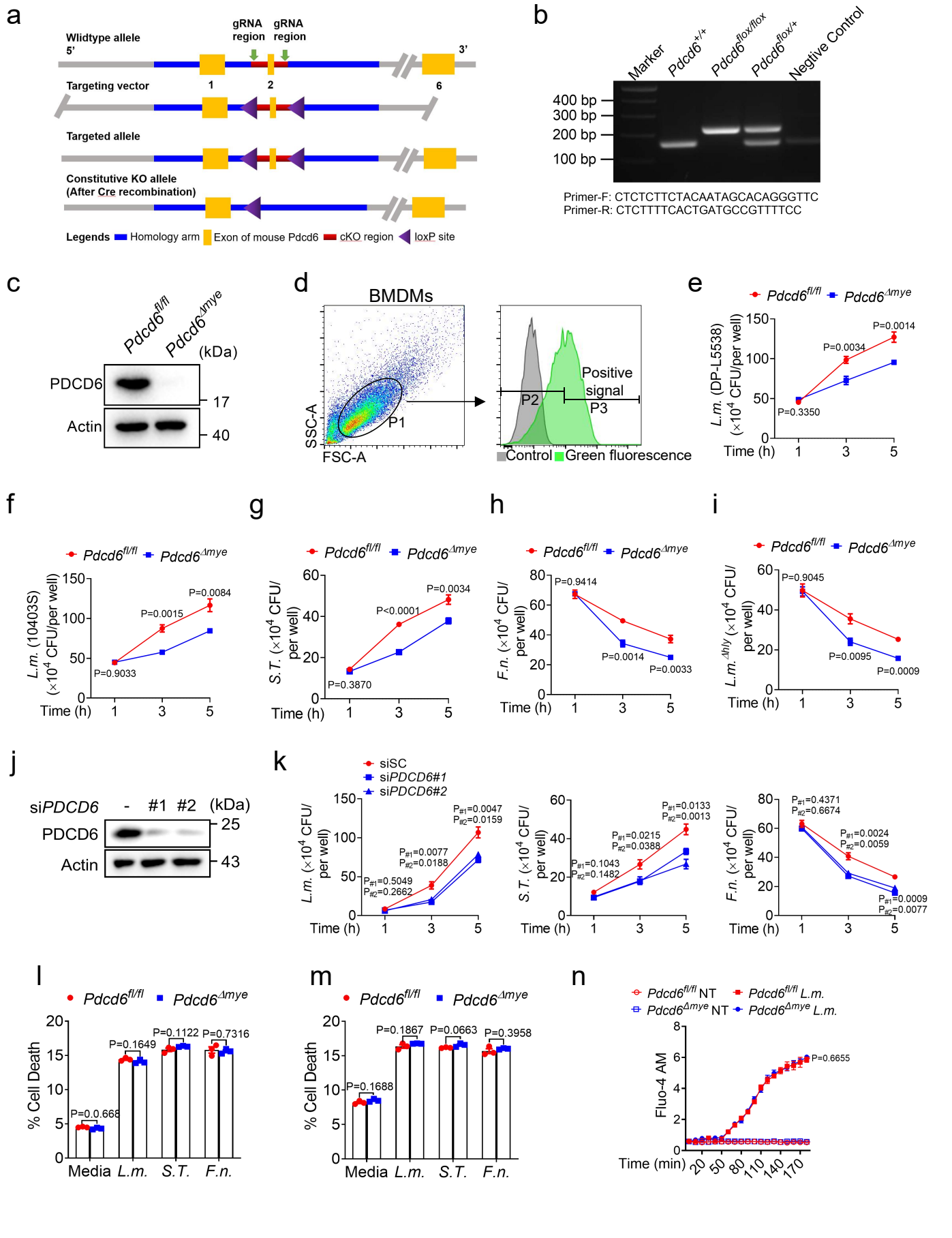
a
Wildtype allele
5'
gRNA region
gRNA region
3'
Targeting vector
1
2
6
Targeted allele
Constitutive KO allele
(After Cre recombination)
Legends Homology arm Exon of mouse Pdcd6 cKO region loxP site
b
Marker
Pdcd6+/+
Pdcd6flox/flox
Pdcd6flox/+
Negtive Control
400 bp
300 bp
200 bp
100 bp
Primer-F: CTCTCTTCTACAATAGCACAGGGTTC
Primer-R: CTCTTTTCACTGATGCCGTTTTCC
c
Pdcd6fl/fl
Pdcd6Δmye
(kDa)
PDCD6
17
Actin
40
d
BMDMs
SSC-A
FSC-A
P1
P2
P3
Positive signal
Control
Green fluorescence
e
Pdcd6fl/fl
Pdcd6Δmye
L.m. (DP-L5538) (×10^4 CFU/per well)
P=0.0014
P=0.0034
P=0.3350
Time (h)
f
Pdcd6fl/fl
Pdcd6Δmye
L.m. (10403S) (×10^4 CFU/per well)
P=0.0084
P=0.0015
P=0.9033
Time (h)
g
Pdcd6fl/fl
Pdcd6Δmye
S.T. (×10^4 CFU/per well)
P=0.0034
P<0.0001
P=0.3870
Time (h)
h
Pdcd6fl/fl
Pdcd6Δmye
F.n. (×10^4 CFU/per well)
P=0.9414
P=0.0014
P=0.0033
Time (h)
i
Pdcd6fl/fl
Pdcd6Δmye
L.m.Δhly (×10^4 CFU/per well)
P=0.9045
P=0.0095
P=0.0009
Time (h)
j
siPDCD6
-
#1
#2
(kDa)
PDCD6
25
Actin
43
k
siSC
siPDCD6#1
siPDCD6#2
L.m. (×10^4 CFU/per well)
P#1=0.0047
P#2=0.0159
P#1=0.0077
P#2=0.0188
P#1=0.5049
P#2=0.2662
S.T. (×10^4 CFU/per well)
P#1=0.0133
P#2=0.0013
P#1=0.0215
P#2=0.0388
P#1=0.1043
P#2=0.1482
F.n. (×10^4 CFU/per well)
P#1=0.4371
P#2=0.6674
P#1=0.0024
P#2=0.0059
P#1=0.0009
P#2=0.0077
Time (h)
l
Pdcd6fl/fl
Pdcd6Δmye
% Cell Death
P=0.0.668
P=0.1649
P=0.1122
P=0.7316
Media
L.m.
S.T.
F.n.
m
Pdcd6fl/fl
Pdcd6Δmye
% Cell Death
P=0.1688
P=0.1867
P=0.0663
P=0.3958
Media
L.m.
S.T.
F.n.
n
Pdcd6fl/fl NT
Pdcd6fl/fl L.m.
Pdcd6Δmye NT
Pdcd6Δmye L.m.
Fluo-4 AM
P=0.6655
Time (min)

Supplementary Fig. 1 Deficiency of PDCD6 increases bacterial killing in cells.
a Graphic of the strategy to generate myeloid-specific *Pdcd6* deletion mice. **b** Genotyping result for indicated mice and the primers used for genotyping. **c** Immunoblotting of PDCD6 in *Pdcd6*$^{fl/fl}$ and *Pdcd6*$^{\Delta mye}$ mice. **d,** Gating strategy to detect green fluorescence signal in BMDMs. Live cells were gated based on forward scatter area (FSC-A) and side scatter area (SSC-A), establishing the P1 gate. A subset of P1 gates was identified using FITC-A, with subset P2 serving as the blank control gate and subset P3 representing the positive signal gate. **e-i** Gentamicin protection assays on *Pdcd6*$^{fl/fl}$ and *Pdcd6*$^{\Delta mye}$ peritoneal macrophages infected with *L. monocytogenes* (DP-L5538) (MOI, 5) (**e**), *L. monocytogenes* (10403S) (MOI, 5) (**f**), *S. Typhimurium* (MOI, 5) (**g**), *F. novicida* (MOI, 20) (**h**) and *L. monocytogenes Δhly* (10403S) (**i**), respectively. **j** Protein expression of PDCD6 in si*PDCD6* #1 and si*PDCD6* #2 THP-1 cells. **k** Gentamicin protection assays on siCtrl and si*PDCD6* THP-1 cells infected with *L. monocytogenes* (DP-L5538) (MOI, 5), *S. Typhimurium* (MOI, 5), and *F. novicida* (MOI, 20), respectively. **l-m** Percentage of cell death in *Pdcd6*$^{fl/fl}$ and *Pdcd6*$^{\Delta mye}$ BMDMs (**l**) or peritoneal macrophages (**m**) infected with indicated bacteria. **n** *Pdcd6*$^{fl/fl}$ and *Pdcd6*$^{\Delta mye}$ BMDMs were incubated with Fluo-4, followed by *L. monocytogenes* (MOI, 5) challenge. The fluorescence signal was read using a microplate reader. The averages of $n = 6$ (**e-i, k**), $n = 3$ (**l**, **m**), $n = 4$ (**n**) biologically independent samples are shown. Data are shown as the mean ± SEM. Statistical significance was determined using *t*-test (and nonparametric tests) (**e-i, l-n**) and Two-way ANOVA (multiple comparisons) (**k**). The presented data are representative of three independent experiments (**b-n**).

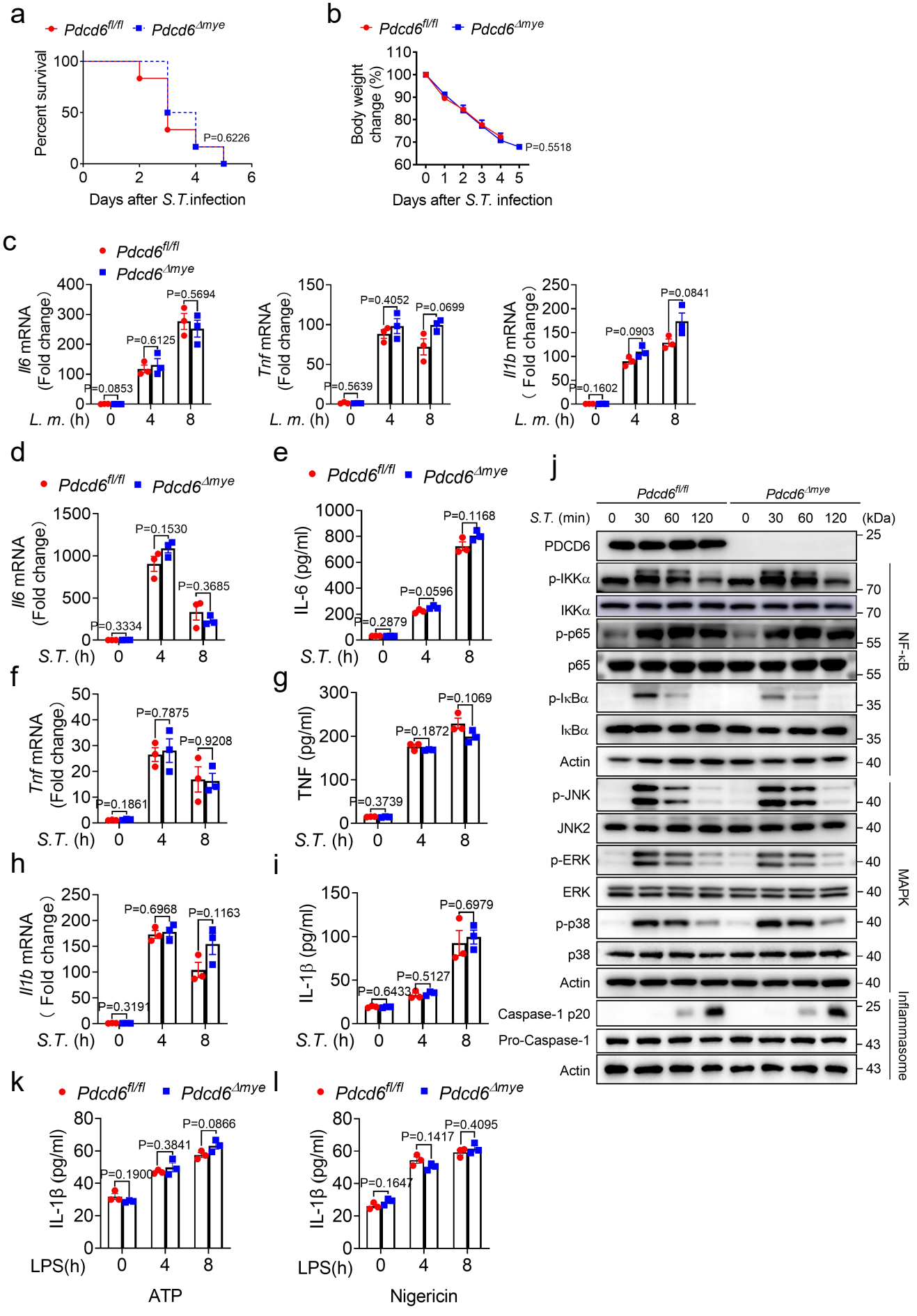
a
Pdcd6fl/fl
Pdcd6Δmye
Percent survival
100
50
0
P=0.6226
0
2
4
6
Days after S.T.infection
b
Pdcd6fl/fl
Pdcd6Δmye
Body weight change (%)
110
100
90
80
70
60
P=0.5518
0 1 2 3 4 5
Days after S.T. infection
c
Pdcd6fl/fl
Pdcd6Δmye
Il6 mRNA (Fold change)
P=0.0853
P=0.6125
P=0.5694
L. m. (h) 0 4 8
Tnf mRNA (Fold change)
P=0.5639
P=0.4052
P=0.0699
L. m. (h) 0 4 8
Il1b mRNA (Fold change)
P=0.1602
P=0.0903
P=0.0841
L. m. (h) 0 4 8
d
Pdcd6fl/fl
Pdcd6Δmye
Il6 mRNA (Fold change)
P=0.3334
P=0.1530
P=0.3685
S.T. (h) 0 4 8
e
Pdcd6fl/fl
Pdcd6Δmye
IL-6 (pg/ml)
P=0.2879
P=0.0596
P=0.1168
S.T. (h) 0 4 8
f
Tnf mRNA (Fold change)
P=0.1861
P=0.7875
P=0.9208
S.T. (h) 0 4 8
g
TNF (pg/ml)
P=0.3739
P=0.1872
P=0.1069
S.T. (h) 0 4 8
h
Il1b mRNA (Fold change)
P=0.3191
P=0.6968
P=0.1163
S.T. (h) 0 4 8
i
IL-1β (pg/ml)
P=0.6433
P=0.5127
P=0.6979
S.T. (h) 0 4 8
j
Pdcd6fl/fl
Pdcd6Δmye
S.T. (min) 0 30 60 120 0 30 60 120 (kDa)
PDCD6 25
p-IKKα 70
IKKα 70
p-p65 55
p65 55
p-IκBα 35
IκBα 35
Actin 40
NF-κB
p-JNK 40
JNK2 40
p-ERK 40
ERK 40
p-p38 40
p38 40
Actin 40
MAPK
Caspase-1 p20 25
Pro-Caspase-1 43
Actin 43
Inflammasone
k
Pdcd6fl/fl
Pdcd6Δmye
IL-1β (pg/ml)
P=0.1900
P=0.3841
P=0.0866
LPS(h) 0 4 8
ATP
l
Pdcd6fl/fl
Pdcd6Δmye
IL-1β (pg/ml)
P=0.1647
P=0.1417
P=0.4095
LPS(h) 0 4 8
Nigericin

Supplementary Fig. 2 *Pdcd6* deficiency attenuates bacterial growth without affecting cytokine production.
a, b Survival (**a**) and body weight change (**b**) of *Pdcd6*$^{fl/fl}$ and *Pdcd6*$^{\Delta mye}$ mice (n = 6, 3 male and 3 female for each group) after intraperitoneal injection with *S. Typhimurium* (0.5×10^6 c.f.u). **c-i** Gene transcripts in the cells (**c**, **d, f, h**) and cytokines in the supernatants (**e, g, i**) from *Pdcd6*$^{fl/fl}$ and *Pdcd6*$^{\Delta mye}$ BMDMs left untreated or stimulated with *L. monocytogenes* (MOI, 5) (**c**) or *S. Typhimurium* (MOI, 5) (**d-i**) for indicated periods. **j** NF-κB, MAPK, and inflammasome activation signaling molecules in *Pdcd6*$^{fl/fl}$ and *Pdcd6*$^{\Delta mye}$ BMDMs left untreated or stimulated with *S. Typhimurium* (MOI, 5) for indicated periods. **k-l** IL-1β in the supernatants from *Pdcd6*$^{fl/fl}$ and *Pdcd6*$^{\Delta mye}$ BMDMs left untreated or stimulated with LPS (100 ng/ml) and further stimulated with ATP (5 mM) (**k**) or nigericin (10 μM) (**l**) for indicated periods. The averages of n = 3 (**c-i**, **k**, **l**) biologically independent samples are shown. Data are shown as the mean ± SEM. Statistical significance was determined using t-test (and nonparametric tests) (**a-i**, **k**, **l**). The presented data are representative of three independent experiments (**a-l**).

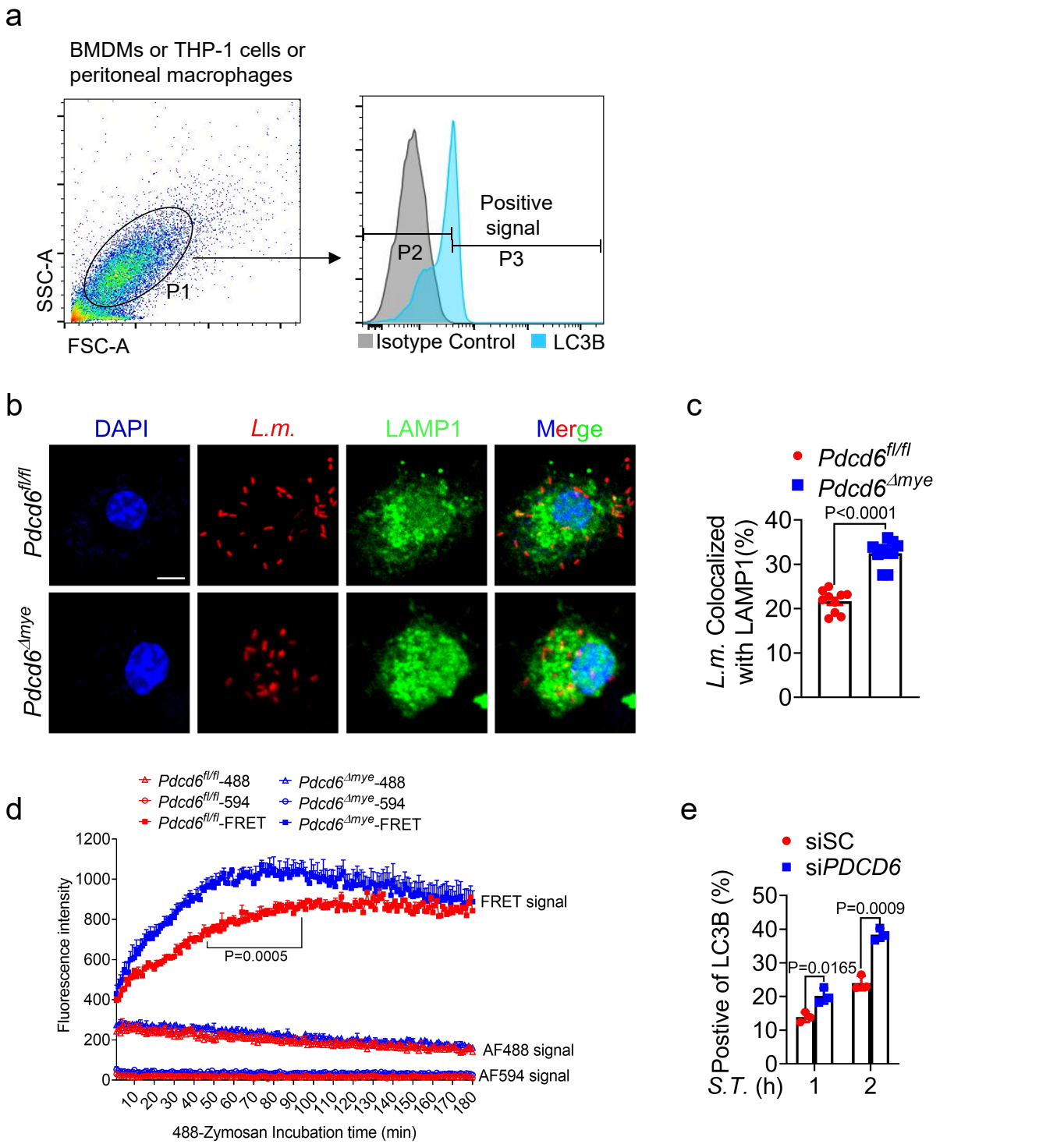

Supplementary Fig. 3 PDCD6 modulates phagosome-lysosome fusion.
a Gating strategy to detect LC3B level in BMDMs. Live cells were gated based on forward scatter area (FSC-A) and side scatter area (SSC-A), establishing the P1 gate. A subset of P1 gates was identified using FITC-A, with subset P2 serving as the blank control gate and subset P3 representing the positive signal gate. **b, c** Confocal images (**b**) and quantification (**c**) of the colocalization between *L. monocytogenes* (red) and LAMP1 (green) in *Pdcd6*$^{fl/fl}$ and *Pdcd6*$^{\Delta mye}$ BMDMs. Scale bar, 2 μm. **d** FRET analysis of the fusion of phagosomes and lysosomes in *Pdcd6*$^{fl/fl}$ and *Pdcd6*$^{\Delta mye}$ BMDMs. **e** Flow cytometry analysis of LC3 fluorescence signal in siCtrl and si*PDCD6* THP-1 cells infected with *S. Typhimurium* (MOI, 5) for indicated periods. The averages of $n = 10$ (**c**), $n = 3$ (**d, e**) biologically independent samples are shown. Data are shown as the mean ± SEM. Statistical significance was determined using *t*-test (and nonparametric tests) (**c, d, e**). The presented data are representative of three independent experiments (**b, d, e**).

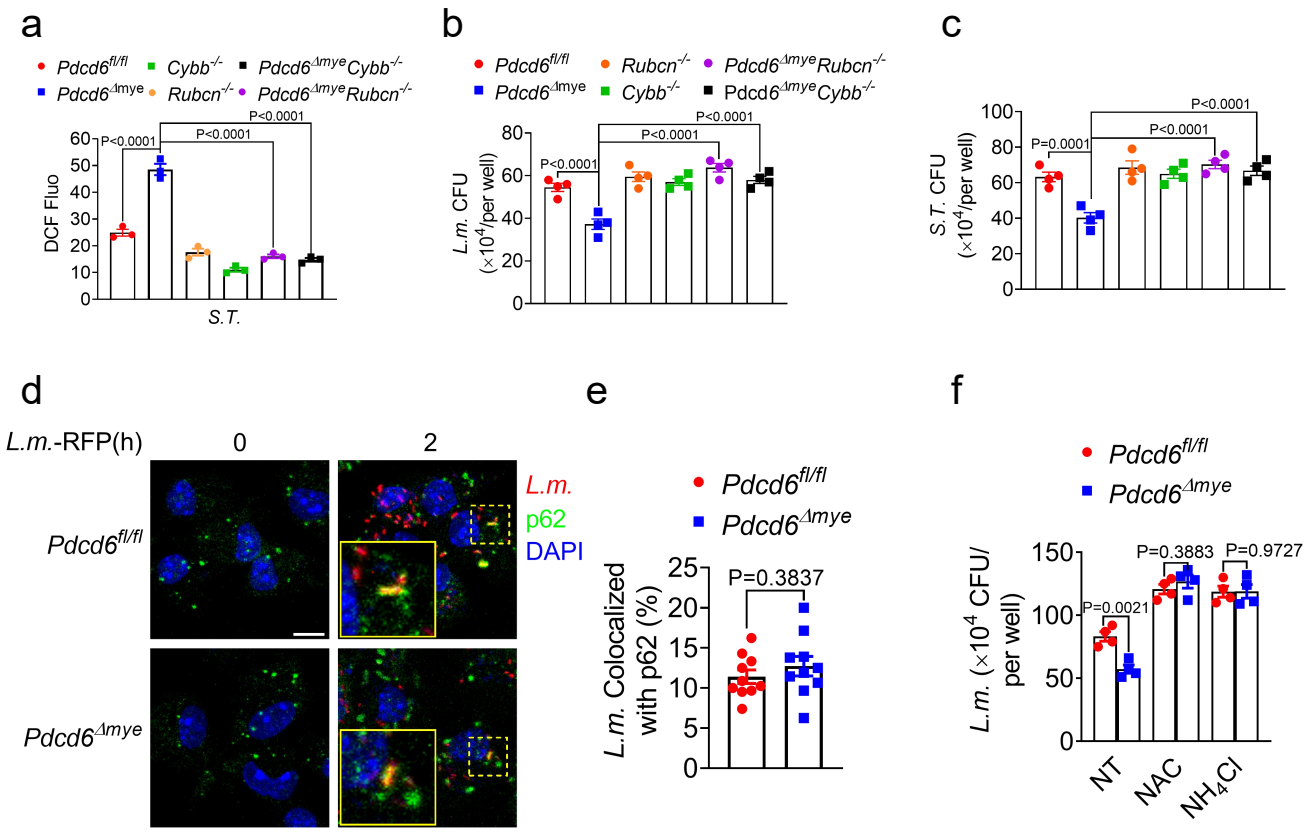

Supplementary Fig. 4 LAP is required for PDCD6 deficiency-enhanced antibacterial immunity.
a ROS production in *Pdcd6*$^{fl/fl}$, *Pdcd6*$^{\Delta mye}$, *Rubcn*$^{-/-}$, *Pdcd6*$^{\Delta mye}$*Rubcn*$^{-/-}$, *Cybb*$^{-/-}$ and *Pdcd6*$^{\Delta mye}$*Cybb*$^{-/-}$ BMDMs infected with *S. Typhimurium*. **b, c** Gentamicin protection assays on indicated BMDMs infected with *L. monocytogenes* (MOI, 5) (**b**) and *S. Typhimurium* (MOI, 5) (**c**) respectively. **d, e** Confocal images (**d**) and quantification (**e**) of the colocalization between *L. monocytogenes* (red) and p62 (green) in *Pdcd6*$^{fl/fl}$ and *Pdcd6*$^{\Delta mye}$ BMDMs. Scale bar, 5 μm. **f** Gentamicin protection assays on given BMDMs infected with *L. monocytogenes* (MOI, 5) pretreated with NAC (5 mM) or NH_4Cl (10 μM) for 4 h. The averages of $n = 3$ (**a**), $n = 4$ (**b, c, f**), $n = 10$ (**e**) biologically independent samples are shown. Data are shown as the mean ± SEM. Statistical significance was determined using One-way ANOVA (multiple comparisons) (**a-c**) and *t*-test (and nonparametric tests) (**e, f**). The presented data are representative of three independent experiments (**a-d, f**).

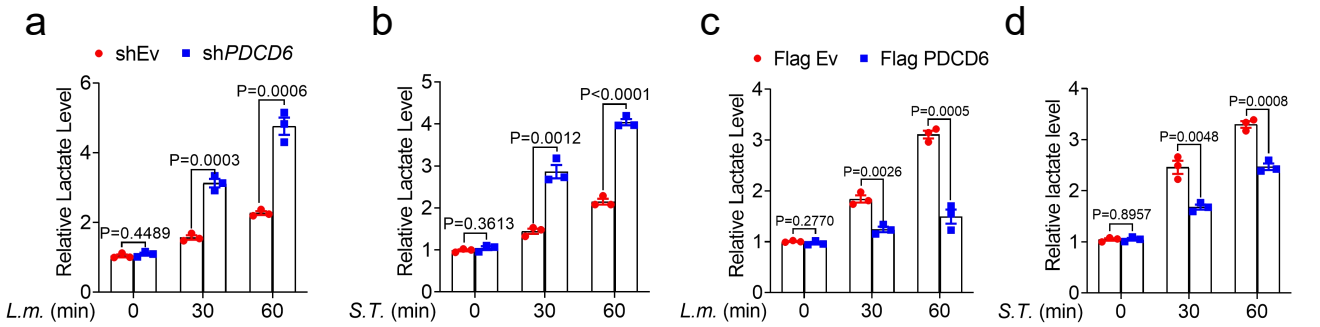

Supplementary Fig. 5 Lactate level increases in PDCD6 deficient cells.
a, b Lactate levels in shCtrl and sh*PDCD6* THP-1 cells treated with *L. monocytogenes* (MOI, 5) (**a**) or *S. Typhimurium* (MOI, 5) (**b**) for indicated periods. **c, d** Lactate levels in PDCD6-overexpressed THP-1 cells treated with *L. monocytogenes* (MOI, 5) (**c**) or *S. Typhimurium* (MOI, 5) (**d**) for indicated periods. The averages of $n = 3$ (**a-d**) biologically independent samples are shown. Data are shown as the mean ± SEM. Statistical significance was determined using *t*-test (and nonparametric tests) (**a-d**). The presented data are representative of three independent experiments (**a-d**).

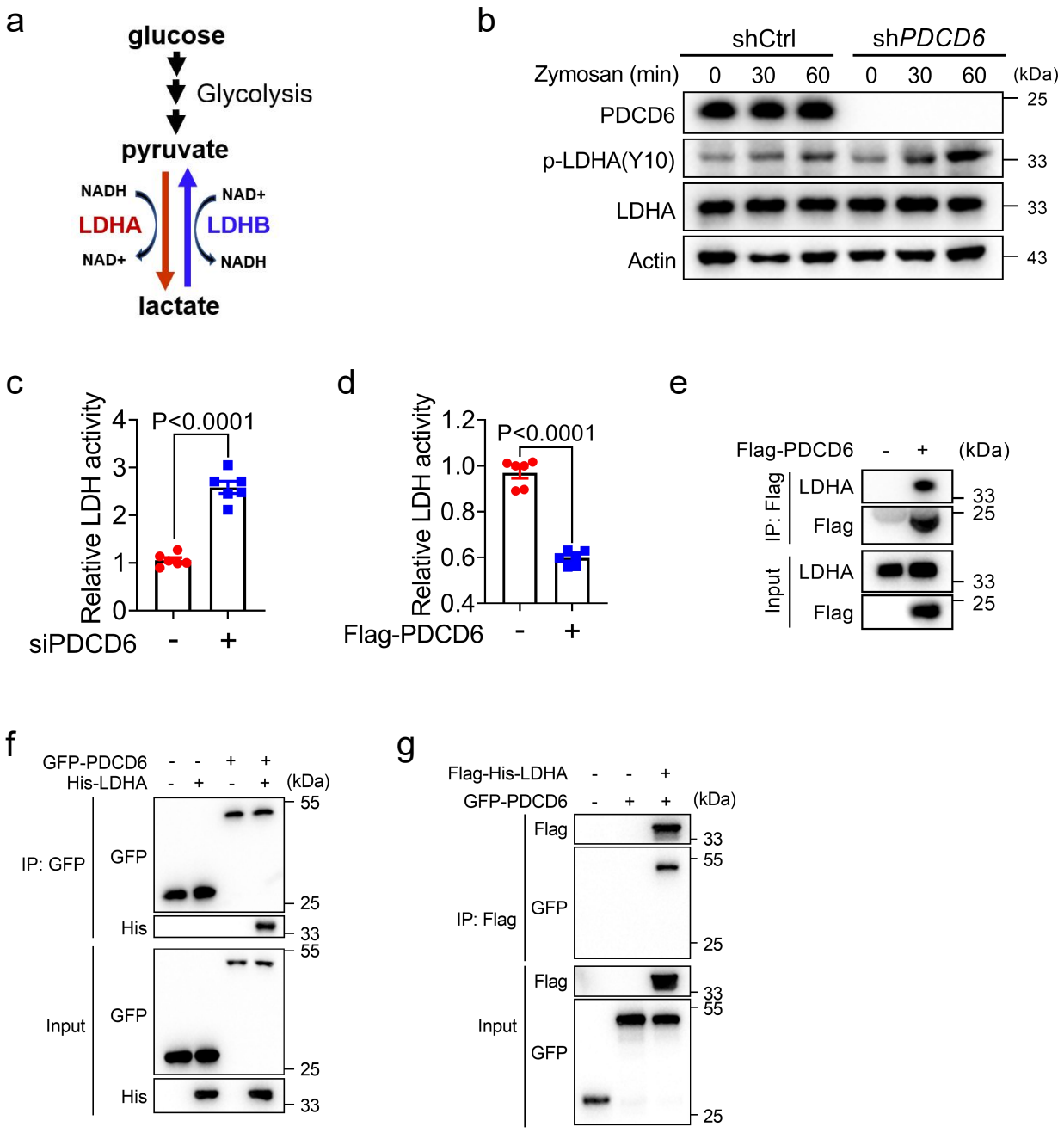

Supplementary Fig. 6 PDCD6 binds to LDHA and modulates its activity.
a Depiction of the metabolic pathway of lactate. **b** Immunoblotting of the expression of given proteins in *Pdcd6*$^{fl/fl}$ and *Pdcd6*$^{\Delta mye}$ BMDMs treated with Zymosan for indicated periods. **c, d** LDH activity in PDCD6-knockdown (**c**) and PDCD6-overexpressed (**d**) THP-1 cells. **e, f, g** 293T cells were transfected for 30 h with the indicated plasmids. Immunoprecipitated proteins were assessed with given antibodies. The averages of $n = 6$ (**c**, **d**) biologically independent samples are shown. Data are shown as the mean ± SEM. Statistical significance was determined using *t*-test (and nonparametric tests) (**c**, **d**). The presented data are representative of three independent experiments (**b-g**).

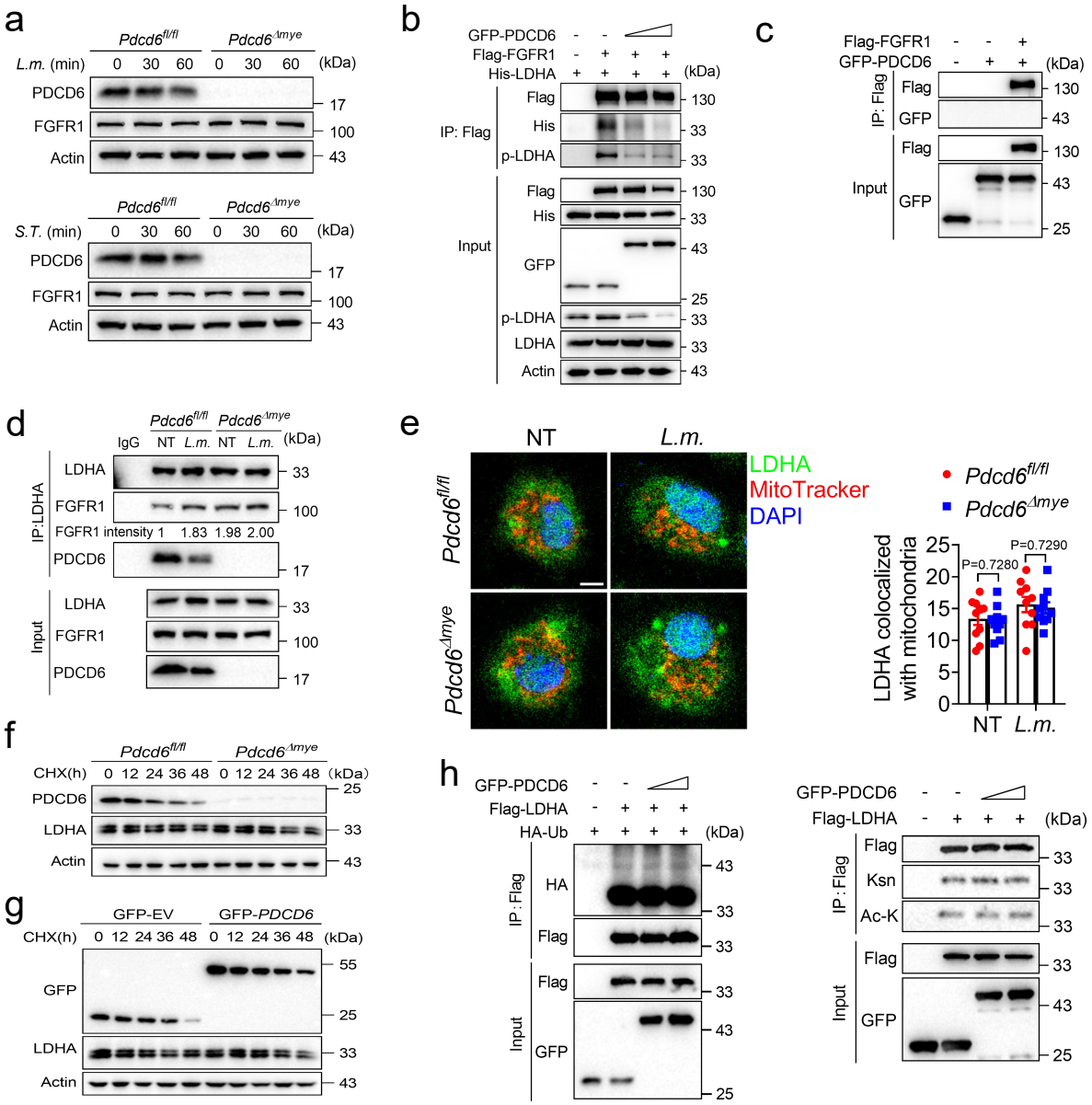

Supplementary Fig. 7 PDCD6 inhibits FGFR1-mediated LDHA activation without affecting its localization or stability.

a The expressions of FGFR1 in *Pdcd6*$^{fl/fl}$ and *Pdcd6*$^{\Delta mye}$ BMDMs left untreated or stimulated with *L. monocytogenes* (MOI, 5) or *S. Typhimurium* (MOI, 5) for indicated periods. **b, c** 293T cells were transfected with the specified plasmids for 30 hours. The immunoprecipitated proteins were then analyzed using the corresponding antibodies. **d** Total LDHA was immunoprecipitated from *Pdcd6*$^{fl/fl}$ and *Pdcd6*$^{\Delta mye}$ BMDMs challenged with or without *L. monocytogenes* (MOI, 5) for 1 hr, followed by immunoblotting with anti-FGFR1 and anti-PDCD6 antibody. **e** Confocal images (**left**) and quantification (**right**) of the colocalization between LDHA (green), mitochondrial (red) and nuclei (blue) in *Pdcd6*$^{fl/fl}$ and *Pdcd6*$^{\Delta mye}$ BMDMs with *L. monocytogenes* challenge or left untreated. Scale bar, 1 μm. **f, g** LDHA stability determined by western blot in *Pdcd6*$^{fl/fl}$ and *Pdcd6*$^{\Delta mye}$ BMDMs (**f**) or PDCD6-overexpressed THP-1 cells (**g**) versus indicated controls. Cells were treated with cycloheximide (CHX) (100 μg/ml) for the given times. **h** 293T cells were transfected with the specified plasmids for 30 hours, followed by immunoprecipitation and antibody-based protein analysis. The averages of $n = 10$ (**e**) biologically independent samples are shown. Data are shown as the mean ± SEM. Statistical significance was determined using *t*-test (and nonparametric tests) (**e**).The presented data are representative of three independent experiments (**a-h**).

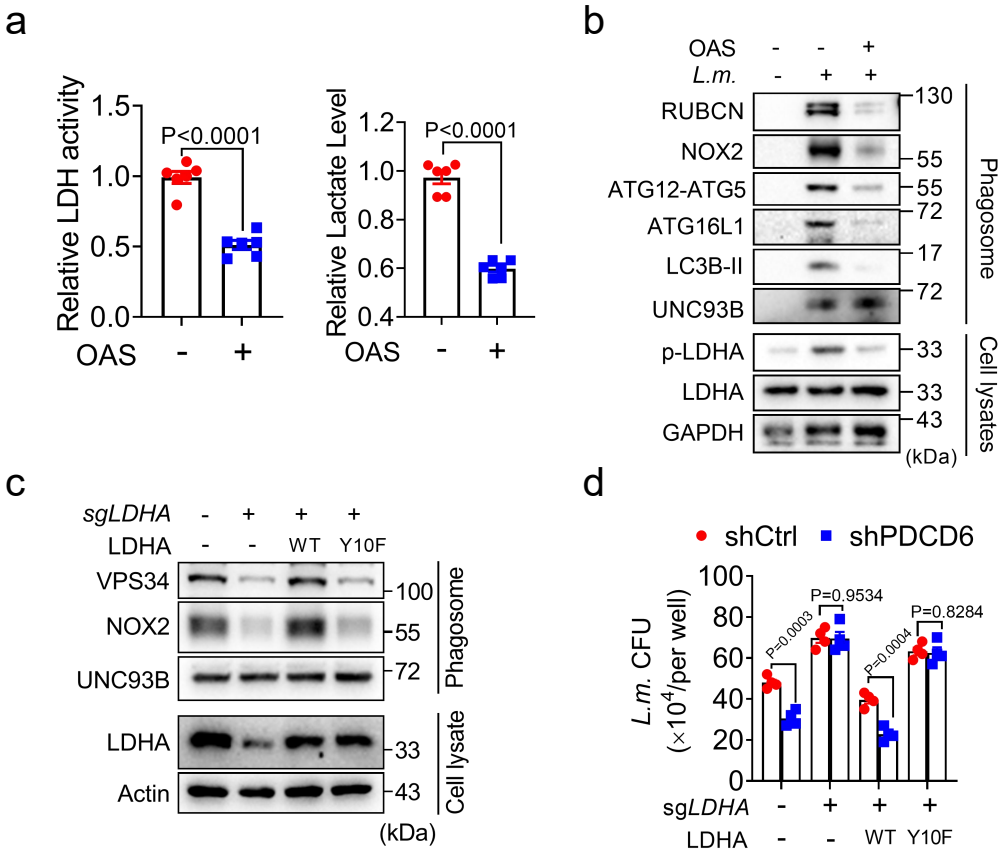

Supplementary Fig. 8 LDHA activity is essential for LAP formation and enhanced bactericidal effect in PDCD6-deficient cells.

a LDH activity and lactate level in BMDMs treated with or without OAS. **b, c** Immunoblotting of LAP-associated molecules in phagosomes and whole cell lysate isolated from BMDMs pretreated with or without OAS **(b)**, or from LDHA-KO THP-1 cells reconstituted with LDHA wild-type or LDHA Y10F **(c)**, followed by *L. monocytogenes* challenge. **d** Gentamicin protection assays on given THP-1 cells infected with *L. monocytogenes*. The averages of n = 6 (**a**), n = 4 (**d**) biologically independent samples are shown. Data are shown as the mean ± SEM. Statistical significance was determined using *t*-test (and nonparametric tests) (**a, d**).The presented data are representative of three independent experiments (**a-d**).

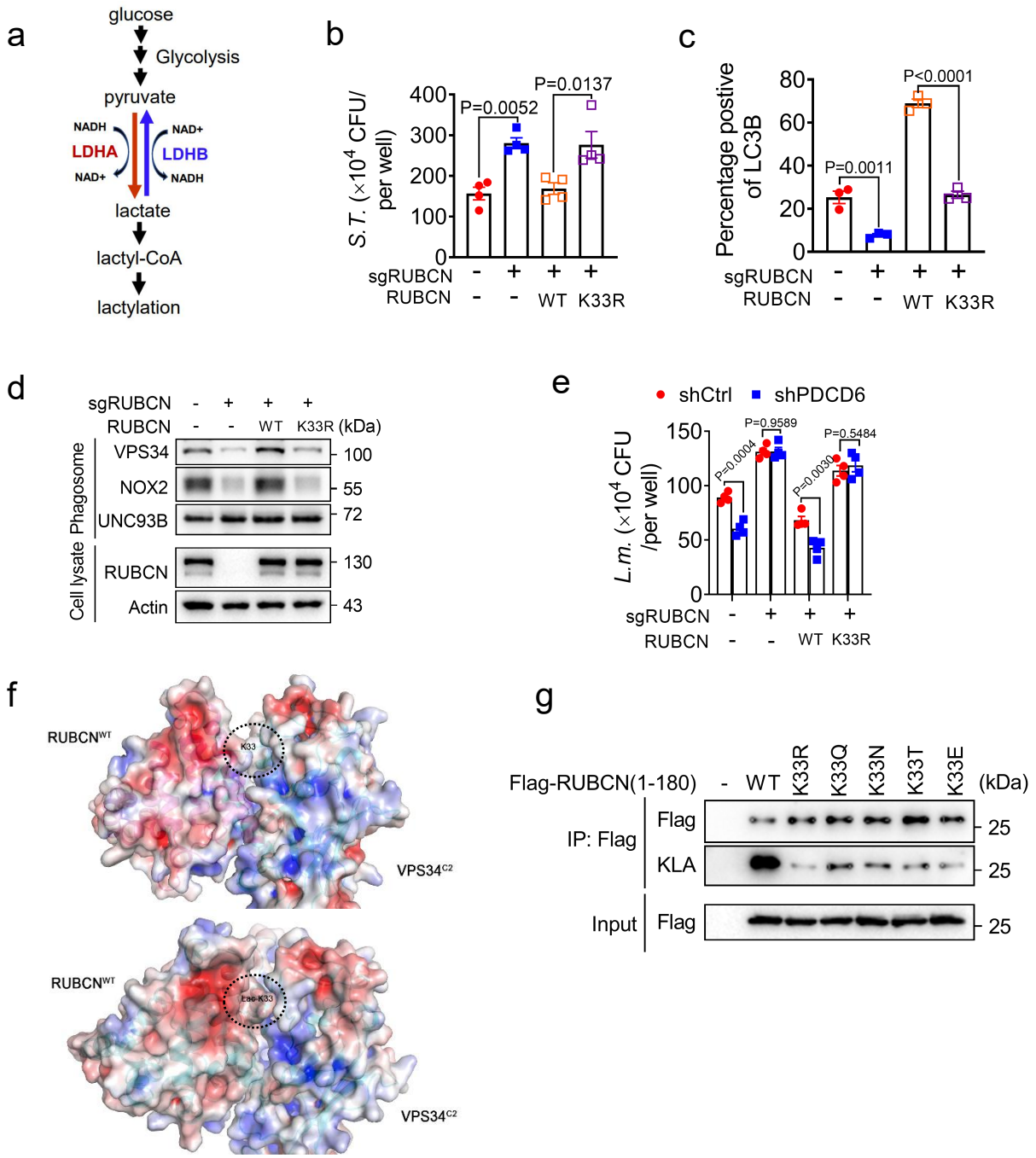

Supplementary Fig. 9 Lactylation of RUBCN enhances bactericidal activity and its interaction with VPS34. **a** Schematic diagram of lactate metabolism. **b, c** Gentamicin protection assays (**b**) and flow cytometry analysis of LC3 fluorescence signal (**c**) on RUBCN KO THP-1 cells with reconstitution of RUBCN WT or K33R mutant followed by *S. Typhimurium* challenge. **d** Immunoblotting of LAP-associated molecules in phagosomes and whole cell lysate isolated from RUBCN KO THP-1 cells with reconstitution of RUBCN WT or K33R mutant followed by *L. monocytogenes* challenge. **e** Gentamicin protection assays on given THP-1 cells infected with *L. monocytogenes*. **f** The surface charge distribution of RUBCN WT system with lactylation (up), RUBCN K33R system (down). The black dash cycles indicate the lactylation site of RUBCN. These complex conformations are all the first frame of MD simulation for each system. **g** 293T cells transfected with the indicated plasmids for 30 h, followed immunoprecipitation assay to detect lactylation. The averages of $n = 4$ (**b, e**), $n = 3$ (**c**), biologically independent samples are shown. Data are shown as the mean ± SEM. Statistical significance was determined using One-way ANOVA (multiple comparisons) (**b**, **c**) and *t*-test (and nonparametric tests) (**e**). The presented data are representative of three independent experiments (**b-e, g**).

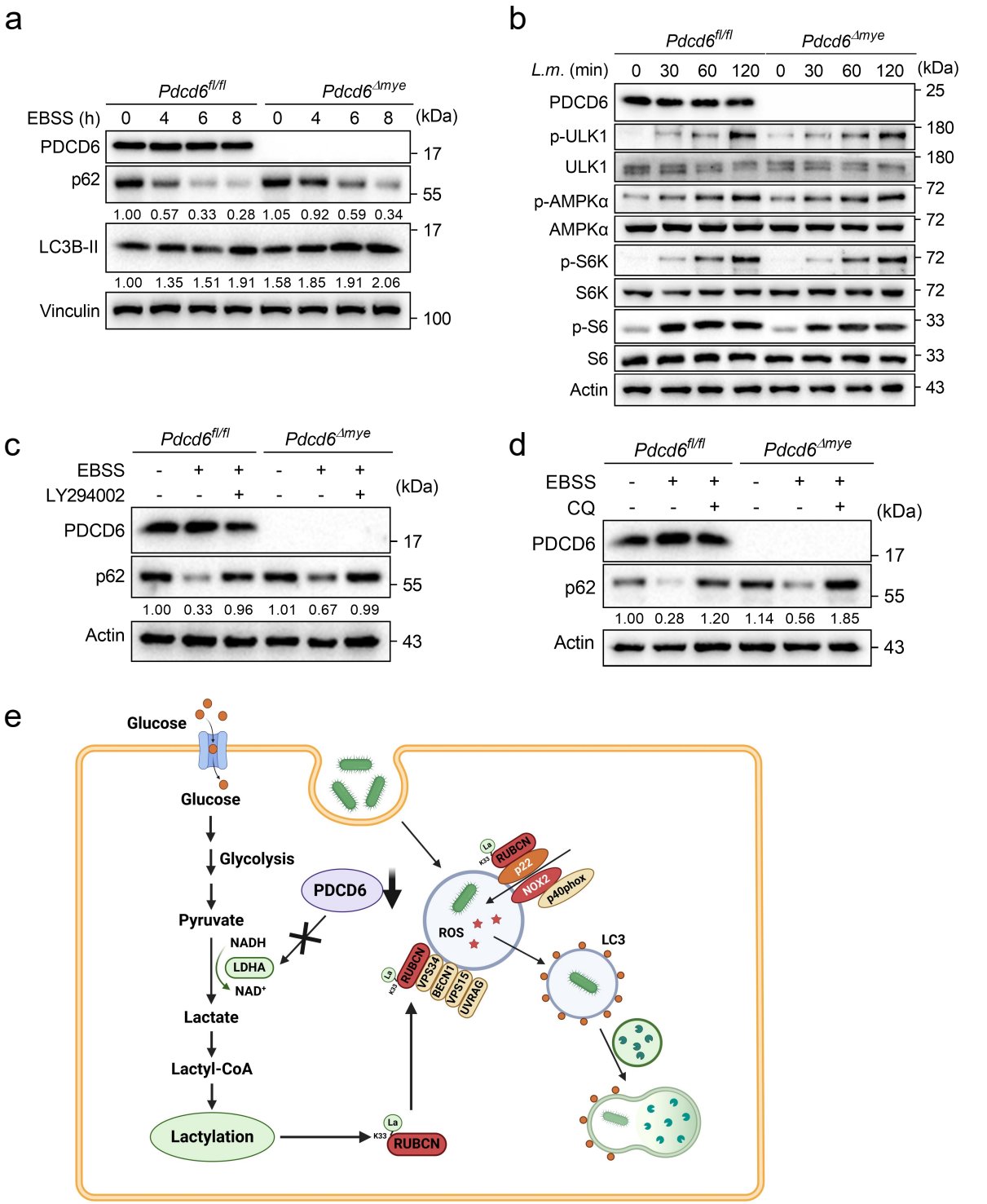

Supplementary Fig. 10 PDCD6 deficiency results in impaired autophagosome maturation.
a Immunoblotting of LC3B and p62 in *Pdcd6*$^{fl/fl}$ and *Pdcd6*$^{\Delta mye}$ BMDMs with EBSS incubation for given times. **b** Immunoblotting of AMPK and mTOR signaling molecules in *Pdcd6*$^{fl/fl}$ and *Pdcd6*$^{\Delta mye}$ BMDMs challenged with *L. monocytogenes* (MOI, 5) for indicated periods. **c, d** Immunoblotting of p62 in *Pdcd6*$^{fl/fl}$ and *Pdcd6*$^{\Delta mye}$ BMDMs with LY294002 (10 μM) (**c**), or Chloroquine (CQ) (5 μM) (**d**) pretreatment for 4 hours, followed EBSS incubation for another 4 hours. **e** Schematic representation of the mechanism of PDCD6 regulating LC3-associated phagocytosis and antibacterial immunity. The illustration was created in BioRender. Lulu, S. (2024) https://BioRender.com/r60a657. The presented data are representative of three independent experiments (**a-d**).

Supplementary Table 1. Differential expressions of Programmed Cell Death (PDCD) family genes left or stimulated with *L. monocytogenes*.

	NT			***L. monocytogenes***			
Gene name	**#1_FPKM**	**#2_FPKM**	**#3_FPKM**	**#1_FPKM**	**#2_FPKM**	**#3_FPKM**	**P value**
Pdcd2	2.602704	3.478187	3.874865	1.707464	1.283281	1.772765	0.013
Pdcd4	1.001026	0.662019	0.901377	1.68305	1.089004	1.025403	0.1516
Pdcd5	2.651803	2.652909	3.092683	1.909768	1.973184	2.143499	0.0083
Pdcd6	47.20366	42.99672	45.92423	37.16613	35.68543	36.84454	0.0026
Pdcd7	5.982611	5.515059	5.07077	4.551977	4.777349	3.320416	0.0672
Pdcd10	14.90303	14.45043	13.56423	17.86296	17.0125	17.47042	0.0025
Pdcd11	9.224934	9.950908	10.54168	6.080339	6.09157	6.331243	0.0007

Supplementary Table 2. Differential metabolites between Non-treated and zymosan-treated groups.

	NT								Zymosan							
Metabolites	***Pdcd6*$^{fl/fl}$**				***Pdcd6*$^{\Delta mye}$**				***Pdcd6*$^{fl/fl}$**				***Pdcd6*$^{\Delta mye}$**			
D-Glucose	1E+05	1E+05	2E+05	1E+05	2E+05	2E+05	2E+05	2E+05	2E+05	1E+05	2E+05	2E+05	2E+05	3E+05	2E+05	2E+05
Glyceraldehyde	28720	32631	30222	29849	33957	36190	33785	35416	31583	34054	33735	34134	41391	43103	46361	43456
Pyruvic acid	59880	66136	68745	64247	78184	76559	71201	72094	72631	77768	74261	71446	83246	86974	92131	81420
Lactate	1E+05	2E+05	2E+05	2E+05	3E+05	3E+05	3E+05	3E+05	3E+05	4E+05	3E+05	4E+05	5E+05	6E+05	5E+05	6E+05
Mannose 6-phosphate	6E+05	7E+05	6E+05	7E+05	1E+06	2E+06	2E+06	1E+06	5E+05	4E+05	5E+05	4E+05	8E+05	9E+05	9E+05	8E+05
Citric acid	20009	20586	20148	21164	90065	77483	79183	84552	22999	22498	24803	26515	82487	81192	79840	82131
α-Ketoglutaric acid	10424	11251	11395	12130	20141	20701	21300	20835	10482	12406	12788	13315	14662	14570	17011	16327
Succinic acid	98182	1E+05	95298	90764	80702	75327	76508	77281	2E+05	2E+05	2E+05	2E+05	1E+05	1E+05	1E+05	1E+05
Malic acid	49277	53038	54512	52573	75295	69394	70792	69531	52289	57066	57038	57905	77816	69312	74543	75619
Oxalic acid	23379	24498	22507	21824	31483	28557	32600	28797	26053	26571	23576	22064	28418	26294	26046	24915
Oxaloacetic acid	12389	12228	12706	11935	14731	15441	13934	14213	12151	13815	13745	13216	16283	17625	19066	16924
Glutamine	3E+06	3E+06	3E+06	3E+06	5E+06	5E+06	5E+06	5E+06	3E+06	4E+06	3E+06	3E+06	4E+06	4E+06	4E+06	4E+06
Glucosamine	79405	58119	70036	61206	70606	77341	54566	91676	98103	79404	95061	86832	78594	90681	74687	81235
UDP-glucose	699.1	1420	890.5	1288	1764	1549	1549	1456	1282	1425	1353	1284	2087	1146	1960	1234

Supplementary Table 3. The binding free energy of $RUBCN^{WT}$ and $RUBCNK^{33R}$

	Energy (kcal/mol)	
Energy Component	**$RUBCN^{WT}$**	**$RUBCN^{K33R}$**
E_{VDW}	-191.7720±11.2556	-153.5329±5.7677
E_{Ele}	-792.2018±71.535	-576.0949±26.9629
E_{GB}	882.3851±67.9718	677.5548±25.5377
E_{Surf}	-28.8035±0.9858	-23.4777±0.7502
ΔG_{gas}	-983.9379±69.0169	-729.6277±26.2965
ΔG_{solv}	853.5816±67.8443	654.0771±25.3899
ΔG	-130.3923±9.5918	-75.5507±10.6949

Supplementary Table 4. Primer sequences for qPCR.

Genes	Forward	Reverse
Mouse *Pdcd6*	TCAGCAAGCATTATCCAATGGT	TCCTGTCTTTATCGACCCTCTG
Mouse *Il6*	AGCTGGAGTCACAGAAGGAG	AGGCATAACGCACTAGGTTT
Mouse *Tnfa*	GTCAGGTTGCCTCTGTCTCA	TCAGGGAAGAGTCTGGAAAG
Mouse *Il1b*	GCAACTGTTCCTGAACTCAACT	ATCTTTTGGGGTCCGTCAACT
Mouse *Marco*	ATGGCACCAAGGGAGACAAAGG	GCCTGGTTTTCCAGCATCACCT
Mouse *Clec7a*	CCAGCTAGGTGCTCATCTACTG	CCTTCACTCTGATTGCGGGAAAG
Mouse *Actb*	AGGGCTATGCTCTCCCTCAC	CTCTCAGCTGTGGTGGTGAA

Supplementary Table 5. Primer sequences for site-directed mutagenesis.

RUBCN(K33R)	Forward	GCAGTTGCTGGGTAATTTGCGGACGACGGTGGAGGGTTTG
	Reverse	CAAACCCTCCACCGTCGTCCGCAAATTACCCAGCAACTGC
RUBCN(K50R)	Forward	AGCCCCAACGTCTGGTCTAGGTATGGTGGCTTGGAGCGGC
	Reverse	GCCGCTCCAAGCCACCATACCTAGACCAGACGTTGGGGCT
RUBCN(K86R)	Forward	TACTGGCAGTTCGTGAGAGACATCCGGTGGCTCAGTCCCC
	Reverse	GGGGACTGAGCCACCGGATGTCTCTCACGAACTGCCAGTA
Flag-RUBCN(K101R)	Forward	AGCCCTTCACGTGGAGAGGTTCATCAGCGTGCACGAGAAC
	Reverse	GTTCTCGTGCACGCTGATGAACCTCTCCACGTGAAGGGCT
RUBCN(K151R)	Forward	CGGGGATAGACAGTATATCAGAAGATTCTACACAGATGCT
	Reverse	AGCATCTGTGTAGAATCTTCTGATATACTGTCTATCCCCG
LDHA(Y10F)	Forward	CTAAAGGATCAGCTGATTTTCAATCTTCTAAAGGAAGAAC
	Reverse	GTTCTTCCTTTAGAAGATTGAAAATCAGCTGATCCTTTAG